Supporting Information

Formation and tuning of pillar porous-layered framework to pillar double-channelled framework

Shuang Liu[a], Chunze Yu[b], Sidan Geng[b] and Jingui Duan[b, c, *]

[a] Henan Engineering Research Center of Green Synthesis for Pharmaceuticals, School of Chemistry & Chemical Engineering, Shangqiu Normal University, Shangqiu 476000, P. R. China.

[b] State Key Laboratory of Chemistry and Utilization of Carbon-Based Energy Resources, College of Chemistry, Xinjiang University, Urumqi, 830000, P. R. China. E-mail: duanjingui@xju.edu.cn

[c] Nanjing Tech University Suzhou Future Membrane Technology Innovation Center, Suzhou 215300, China.

Materials and Characterizations

All reagents and solvents were commercially available and used as received.

1,3,5-tris(2-methyl-1H-imidazol-1-yl) benzene (TMBIB) synthesis. A mixture of 1,3,5-tribromobenzene (1.0 g, 3.2 mmol), anhydrous potassium carbonate (4.0 g, 29.0 mmol), 2-methylimidazole (5.0 g, 61.0 mmol), and copper(II) sulfate (25 mg, 0.156 mmol) was placed in a 50 mL Teflon-lined stainless steel autoclave under a nitrogen atmosphere. The reaction mixture was heated to 185 °C and maintained at this temperature for 48 h. After cooling to ambient temperature, the crude product was sequentially washed with deionized water (3 × 20 mL) to remove inorganic salts. The resulting solid was extracted with dichloromethane (3 × 30 mL), and the combined organic phases were concentrated under reduced pressure to yield ligand **TMBIB** as a brown solid. ^{1}H NMR (400 MHz, $CDCl_3$): d = 2.498 (s, 9H), 7.091 (d, 3H), 7.102 (d, 3H), 7.351 (s, 3H).

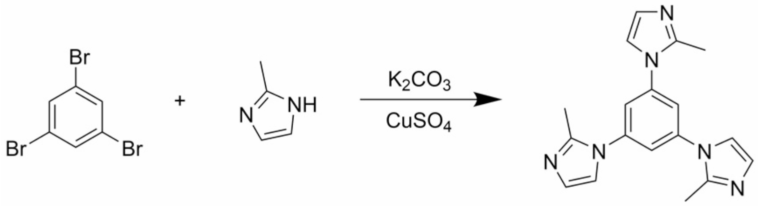

Fig. S1. Synthetic route of the ligand TMBIB

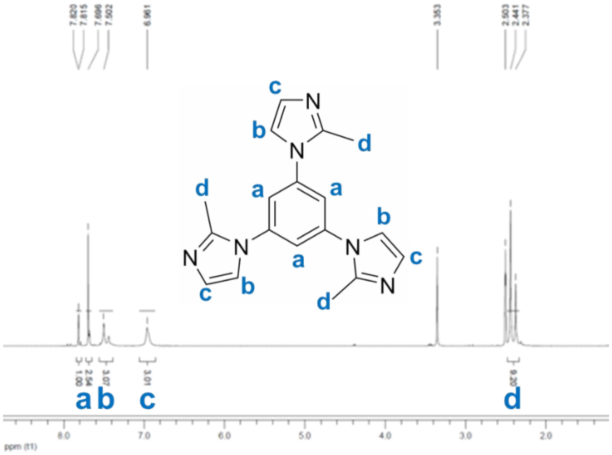

Fig. S2. ^{1}H NMR spectrum of the ligand TMBIB

Synthesis of Cu-TMBIB-a. A solution of copper(II) acetate ($Cu(OAc)_2$, 6.0 mg) and ammonium hexafluorosilicate ($(NH_4)_2SiF_6$, 12.0 mg) in deionized water (0.5 mL) was carefully layered at the bottom of a glass tube (diameter ≈ 0.8 cm). A middle buffer layer of ethanol/water (1.3 mL EtOH and 0.2 mL H_2O) was slowly introduced along the tube wall to minimize mixing. Finally, an ethanol solution (0.5 mL) containing **TMBIB** (5.0 mg) was layered atop the buffer phase. The tube was sealed and stored undisturbed at room temperature for 21 days. Purple block-shaped crystals suitable for X-ray diffraction formed at the interface of the layers. The crystals were isolated by decantation, washed with cold ethanol (3 × 1 mL), and air-dried. **Yield**: ~55% (based on **TMBIB**). The activation process of the material was carried out as follows: The as-synthesized sample was immersed in dry methanol for three days, with fresh solvent replaced every eight hours. After vacuum filtration, the sample was subjected to vacuum heating activation at 120 °C overnight, and then sealed and properly stored.

Synthesis of Cu-TMBIB-b. A solution of copper(II) chloride ($CuCl_2$, 6.0 mg) and ammonium hexafluorotitanate ($(NH_4)_2TiF_6$, 6.0 mg) in deionized water (0.5 mL) was carefully layered at the bottom of a glass tube (diameter ≈ 0.8 cm). A middle buffer layer of *N,N*-dimethylformamide (DMF)/methanol (MeOH)/water (1.3 mL DMF : 0.5 mL MeOH : 0.1 mL H_2O) was slowly introduced along the tube wall to establish a solvent gradient. Finally, a methanol solution (0.5 mL) containing ligand **TMBIB** (5.0 mg) was layered atop the buffer phase. The tube was sealed and stored undisturbed at room temperature for 14 days. Blue block-shaped crystals formed at the solvent interfaces and were collected by decantation, washed with cold ethanol (3 × 1 mL), and air-dried. **Yield**: ~30% (based on **TMBIB**).

Crystallography. Single-crystal X-ray diffraction data was collected by a Rigaku XtaLAB Synergy-DW diffractometer at 298 K using graphite monochromator Mo Kα radiation (λ = 0.71073 Å). Data reduction was made with the CrysAlisPro program. The structure was solved by direct methods and refined with full-matrix least-squares technique using the SHELXTL package.[1] Non-hydrogen atoms were refined with anisotropic displacement parameters during the final cycles. Organic hydrogen atoms were placed in calculated positions with isotropic displacement parameters set to 1.2 × Ueq of the attached atom. The unit cell includes a large region of disordered solvent molecules, which could not be modeled as discrete atomic sites. We employed PLATON/SQUEEZE [2] to calculate the diffraction contribution of the solvent molecules and, thereby, to produce a set of solvent-free diffraction intensities; the structure was then refined again using the data generated. Crystal data are summarized in Table S1.

Characterization. The chemical structure of the TMBIB ligand was confirmed by ^{1}H NMR spectroscopy using a Bruker Advance III 400 MHz spectrometer with $CDCl_3$ as the solvent. The phase purity of the as-synthesized MOFs was verified by powder X-ray diffraction (PXRD) measurements performed on a Bruker AXS D8 Advance diffractometer operating at 40 kV and 40 mA with Cu Kα radiation (λ = 1.5418 Å). Simulated powder patterns from single-crystal X-ray diffraction data were generated using Mercury 1.4.2 software. Thermogravimetric analysis (TGA) was conducted on a NETZSCH STA 209 F1 thermo-microbalance to evaluate the thermal stability of the materials. Samples were heated from room temperature to 800 °C at a heating rate of 10 °C min^{-1} under a continuous nitrogen flow.

Liquid-phase batch adsorption experiments were conducted at ambient temperature to evaluate the iodine capture performance of the MOFs. Typically, vacuum-activated Cu-TMBIB-a (10.0 mg), obtained by heating the as-synthesized material at 120 °C overnight under dynamic vacuum to remove guest solvents, was used as the adsorbent. The adsorbent was introduced into a 5.0 mmol L^{-1} I_2 solution in n-hexane (20.0 mL, containing ~25.4 mg I_2, provided in excess relative to the estimated capacity of the MOF to ensure saturation). The mixture was stirred magnetically (300 rpm) at 25 °C. Adsorption progress was monitored by periodically withdrawing a 0.2 mL aliquot of the supernatant, diluting it 10-fold with n-hexane, and measuring the absorbance at 290 nm (λmax for I_2 in n-hexane) by UV-Vis spectroscopy. Equilibrium was considered reached when the relative deviation in absorbance between three consecutive measurements taken at 2 h intervals was < 3% (i.e., a stable concentration over 6 h); a total adsorption time of 24 h was employed to ensure complete equilibration. The I_2-loaded material (I_2@Cu-TMBIB-a) was then isolated by centrifugation (8000 rpm, 10 min), gently rinsed three times with anhydrous ethanol (~0.5-1 mL per rinse), and dried in vacuo at 60 °C overnight prior to further characterization. The I_2 adsorption capacity was quantitatively determined via X-ray photoelectron spectroscopy (XPS). High-resolution XPS spectra were recorded using a Kratos Axis Ultra DLD spectrometer with Al Kα radiation, and the binding energy scale was calibrated against the C 1s peak. The spectra were deconvoluted to identify iodine species and the adsorption capacity was calculated based on the integrated peak areas of the I 3d signals, combined with the relative sensitivity factor method and elemental mass concentration analysis.

Table S1. Crystal data and structural refinement parameters for **Cu-TMBIB-a** and **Cu-TMBIB-b**.

	Cu-TMBIB-a	**Cu-TMBIB-b**
Empirical formula	$[C_{72}H_{74}Cu_3F_6N_{24}OSi\cdot 2(SiF_6)]\cdot$xSolvent	$[C_{216}H_{216}Cu_{10}F_{30}N_{72}Ti_5]\cdot$xSolvent
Formula Weight	1908.47	1316.37
Crystal System	tetragonal	tetragonal
Space group	*I*4/mcm	*P*4/mnc
dimensions (Å)	*a* = 17.5784(8)	*a* = 44.4981(10)
	b = 17.5784(8)	*b* = 44.4981(10)
	c = 46.063(4)	*c* = 12.9740(6)
Cell Volume (Å^3)	14233.5(18)	25689.6(17)
Z	4	8
Density (g/cm^3)	0.891	0.681
Mu (MoKa) (mm^{-1})	0.528	0.519
$F_{(000)}$	3892	5372
Theta min-max	0.9, 25.0	0.6, 25.0
Index ranges	-20≤ h ≤20	-52≤ h ≤52
	-20≤ k ≤20	-52≤ k ≤52
	-54≤ l ≤54	-14≤ l ≤15
Tot , Uniq Data, *R*(int)	49243, 3351, 0.078	183655, 11914, 0.128
Observed data [*I* > 2σ (I)]	2245	7186
N_{ref}, N_{par}	3351, 182	11914, 683
R_1, wR_2, S	0.0477, 0.0994, 1.034	0.1053, 0.2979, 1.09
Max Shift	0.00	0.00

R = Σ||Fo|-|Fc||/Σ|Fo|, w*R* = {Σ[w(|Fo|2 - |Fc|2)2]/Σ[w(|Fo|4)]}1/2 and *w* = 1/[σ2(Fo2) + (0.1141P)2]

where *P* = (Fo2+2Fc2)/3

Structure details

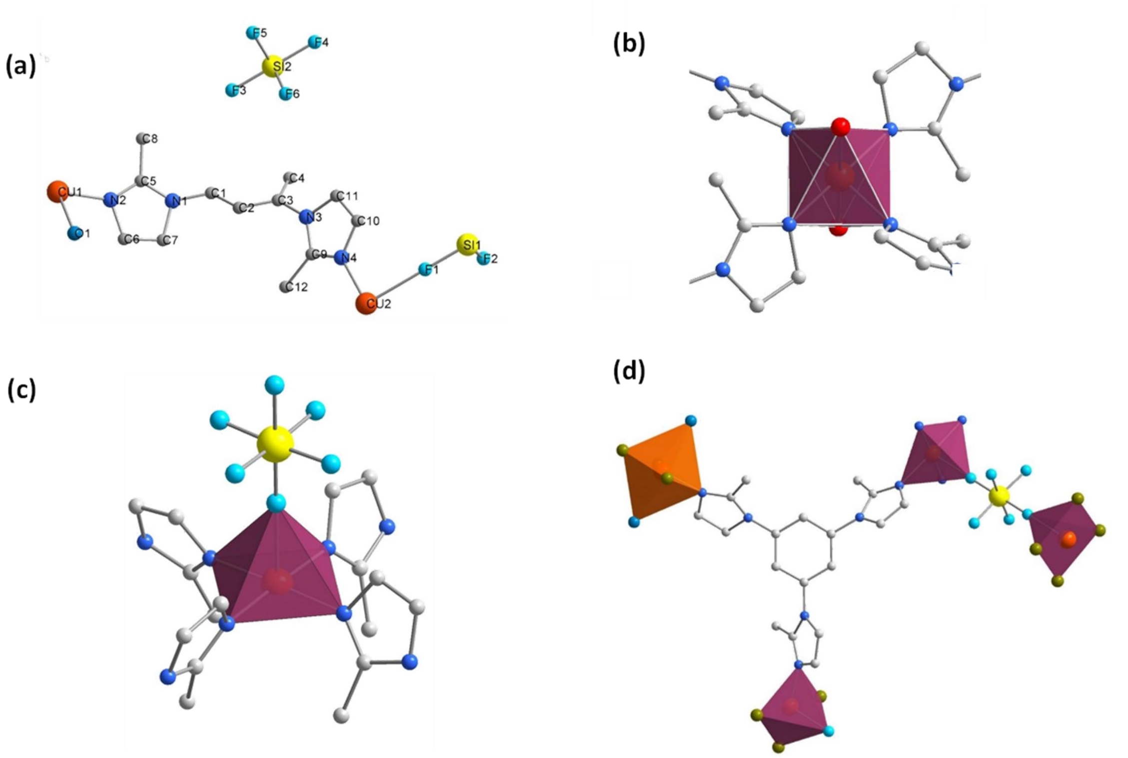

Fig. S3. Structure of **Cu-TMBIB-a**: Asymmetric unit (a), 4-connected Cu1 node (b), 5-connected Cu2 node (c) and the connection of **TMBIB** and SiF_6^{2-} ion (d).

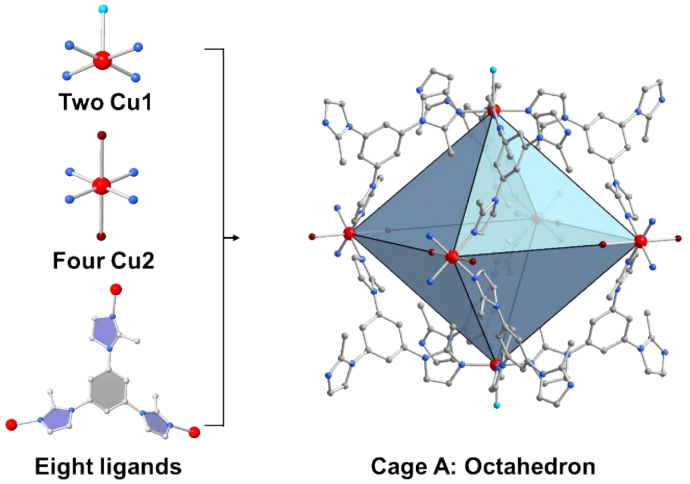

Fig. S4. Structure of **Cu-TMBIB-a**: View of the basic units and the formed octahedral cage A.

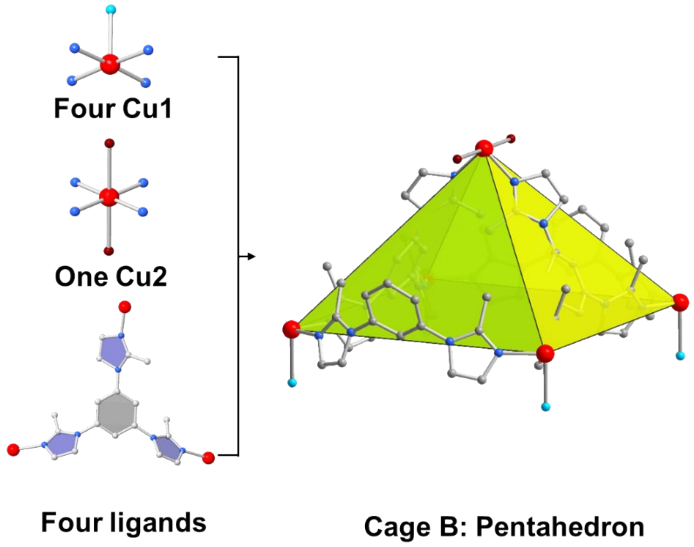

Fig. S5. Structure of **Cu-TMBIB-a**: View of the basic units and the formed pentahedral cage B.

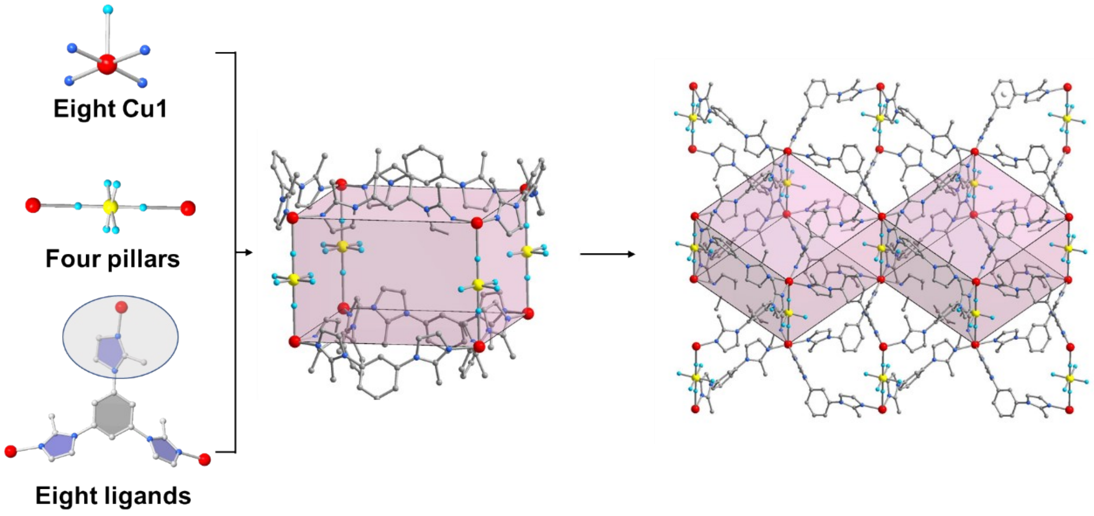

Fig. S6. Structure of **Cu-TMBIB-a**: View of the pillar supported cage C.

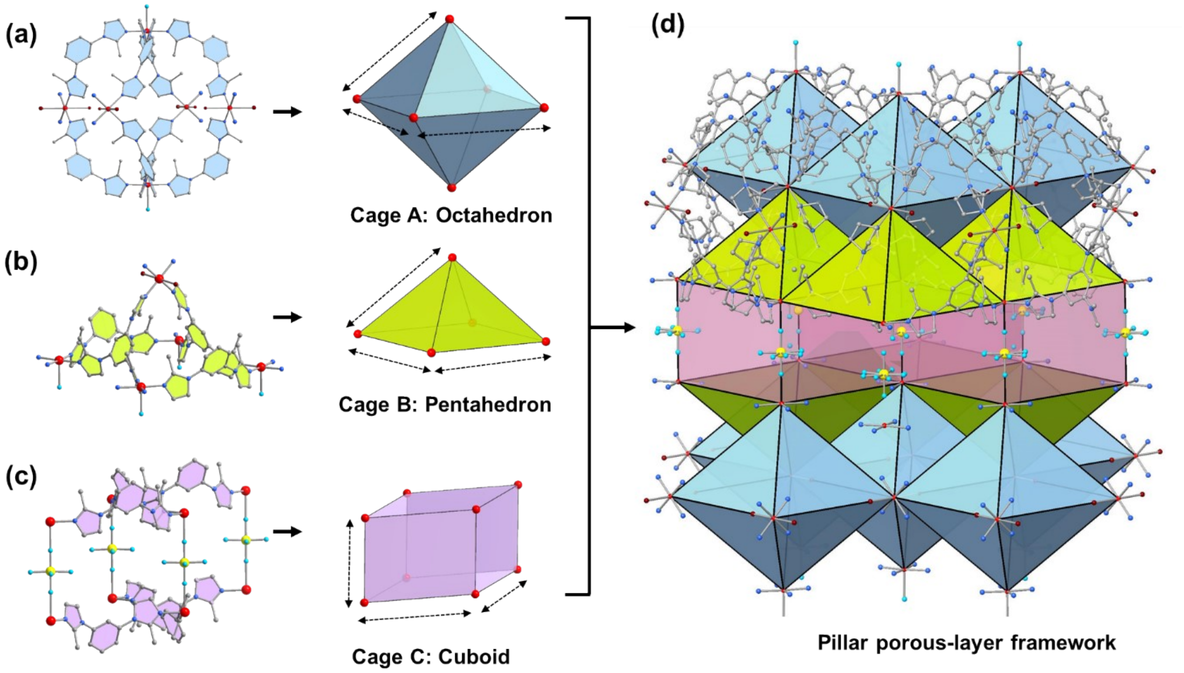

Fig. S7. Structure of **Cu-TMBIB-a**: Pillared porous-layer framework constructed from Three types of cages.

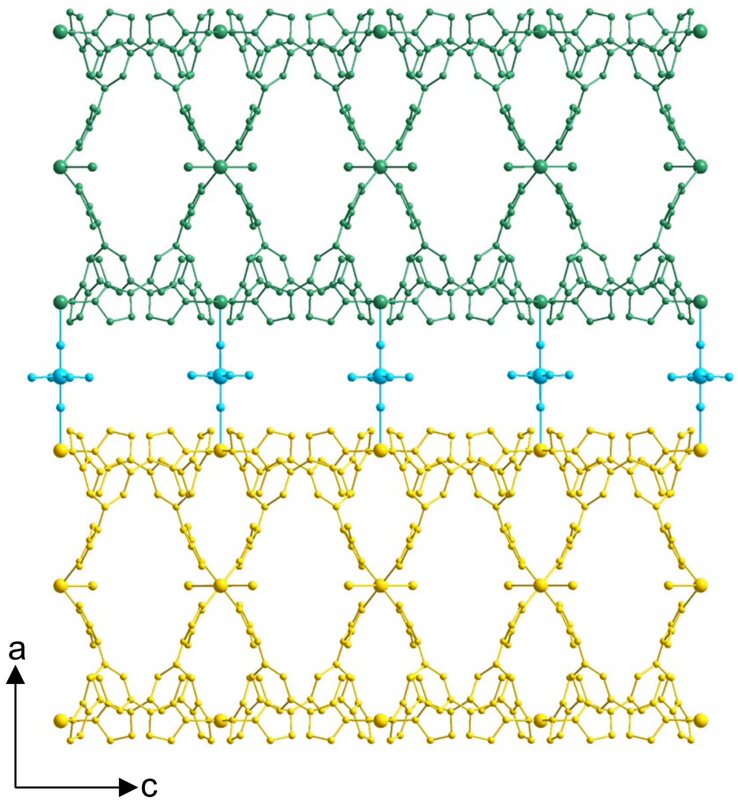

Fig. S8. The arrangement of the pillar-layered **Cu-TMBIB-a** framework.

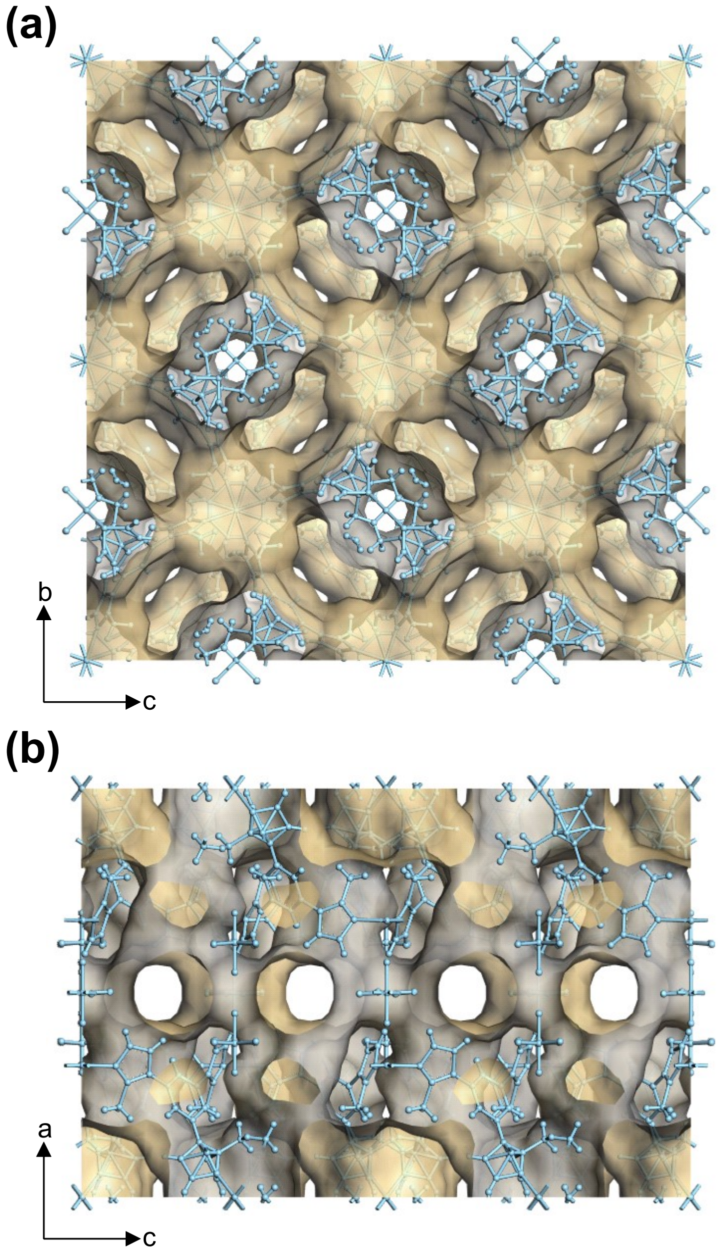

Fig. S9. View of the accessible inner space of **Cu-TMBIB-a** along a-axis (a) and b-axis (b). The radius of the probe is 1.2Å.

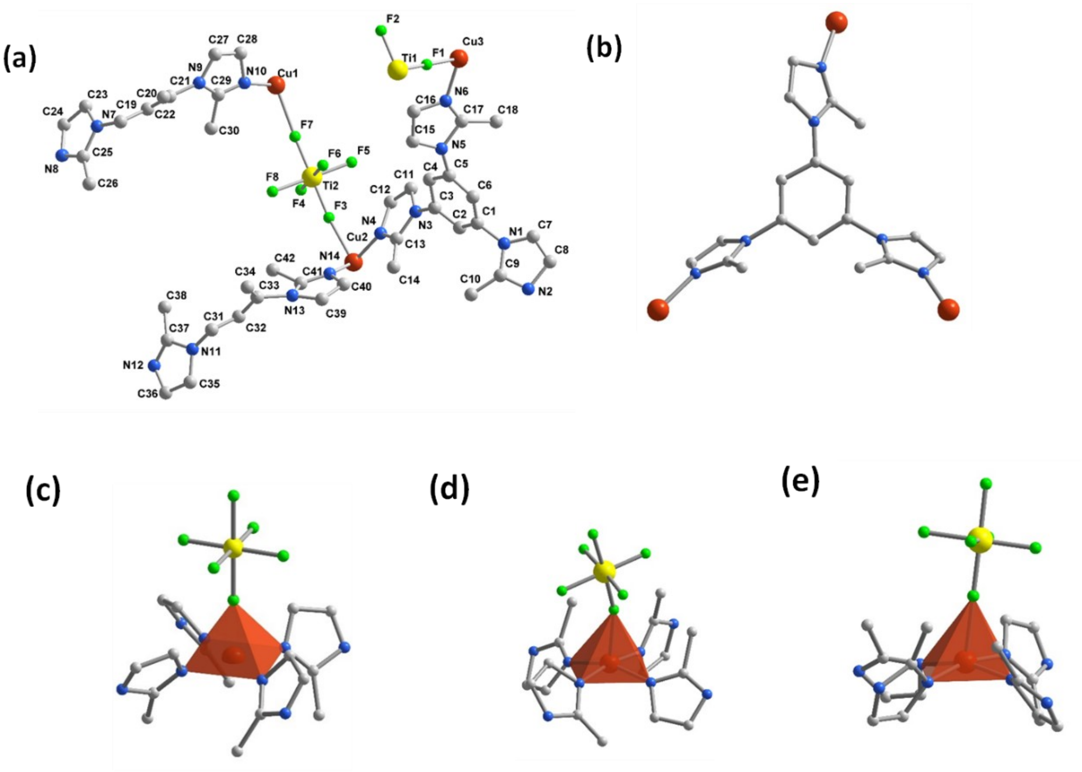

Fig. S10. Structure of **Cu-TMBIB-b**: Asymmetric unit (a), 3-connected **TMBIB** ligand (b), three connection modes of Cu nodes (c-e).

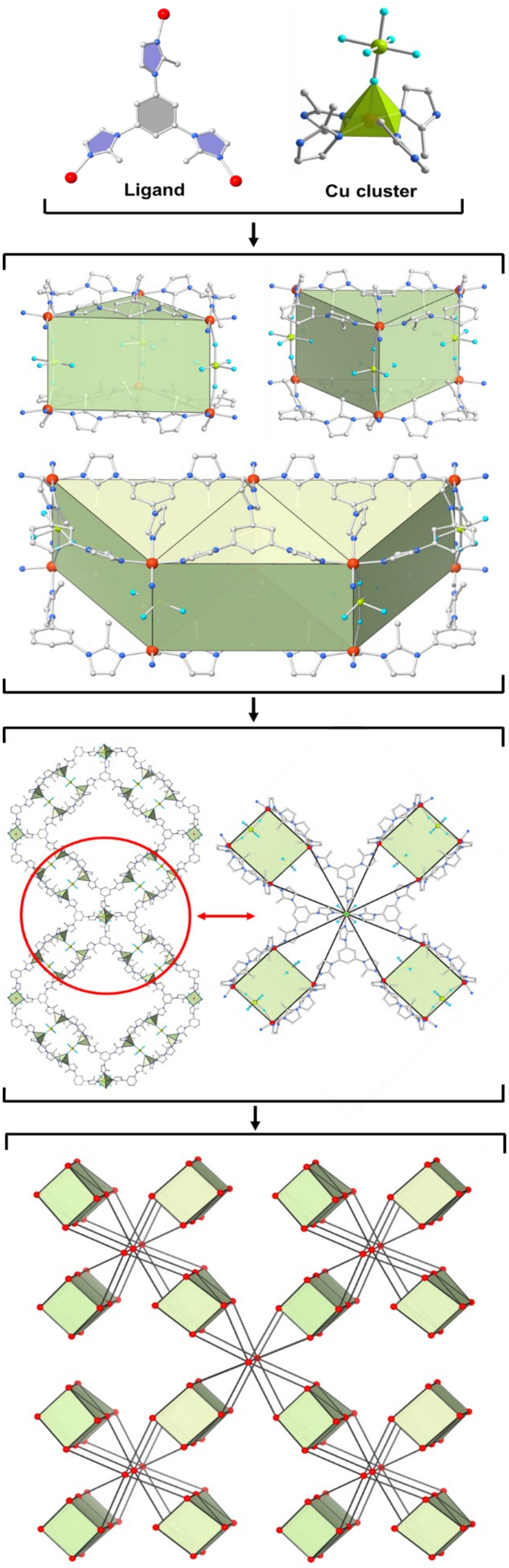

Fig. S11. Illustration of the topology formation of **Cu-TMBIB-b**.

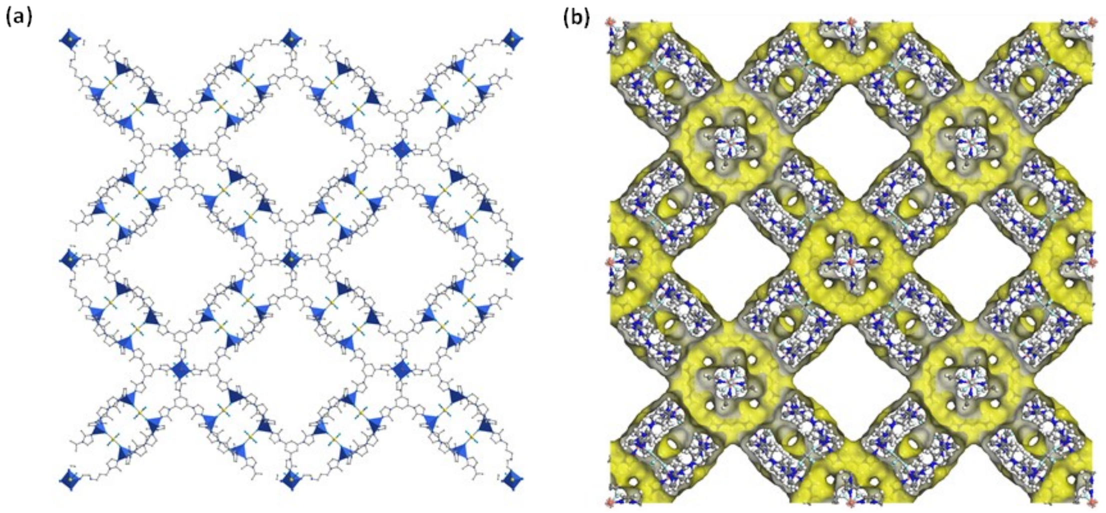

Fig. S12. Views of periodic arrangement of pillar double-channeled units (a) and the channel space (b) of **Cu-TMBIB-b**.

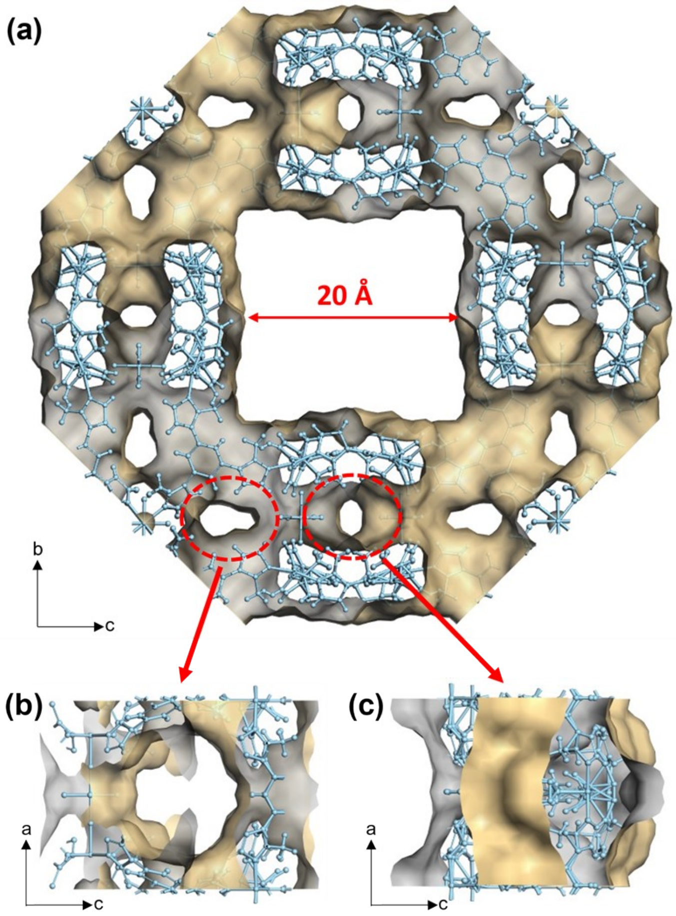

Fig. S13. View of the accessible inner space of **Cu-TMBIB-b** along a-axis (a); two available cage space along b-axis (b) and (c). The radius of the probe is 1.2Å.

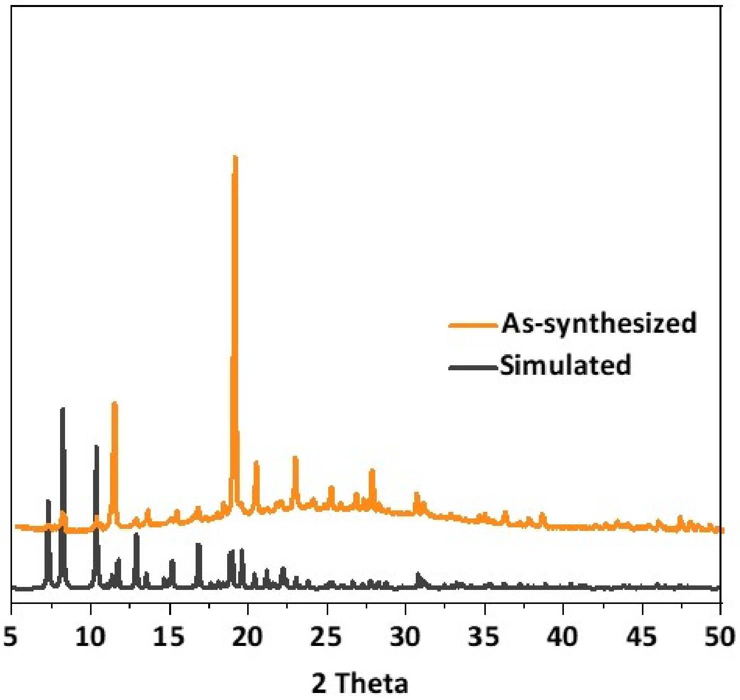

Fig. S14. PXRD of simulated and as-synthesized **Cu-TMBIB-b**.

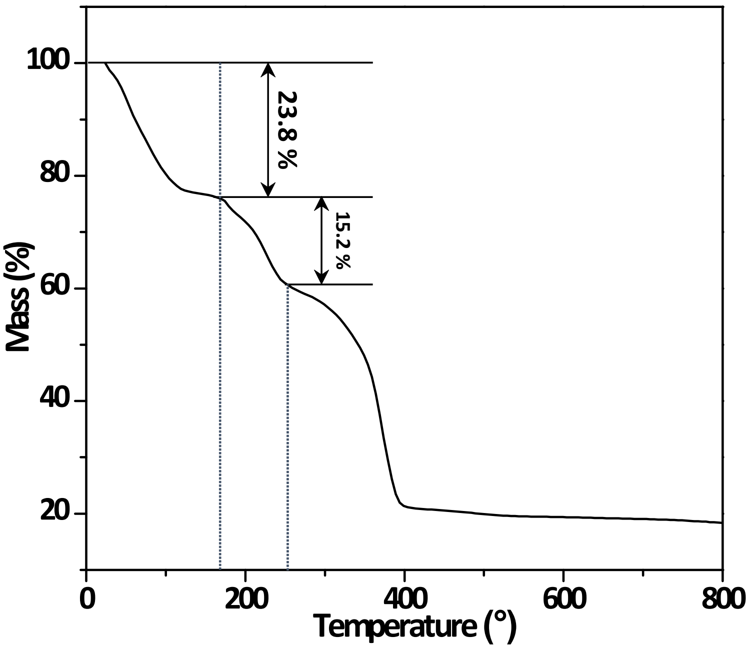

Fig. S15. TGA results of **Cu-TMBIB-a**.

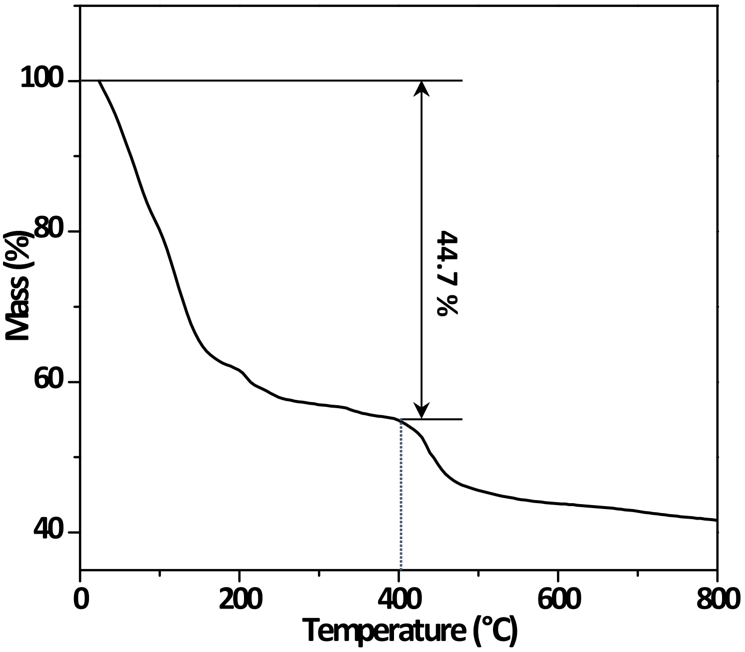

Fig. S16. TGA results of **Cu-TMBIB-b**.

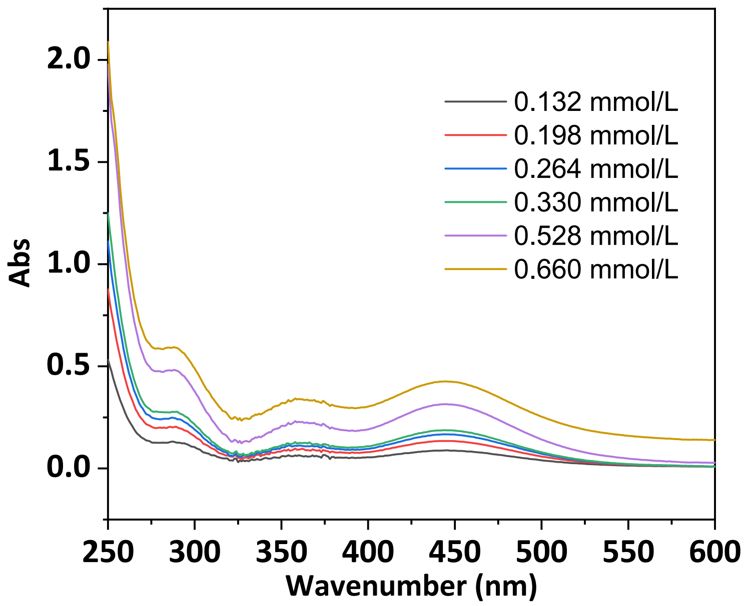

Fig. S17. UV spectra of standard solution of I_2 in ethanol at room temperature.

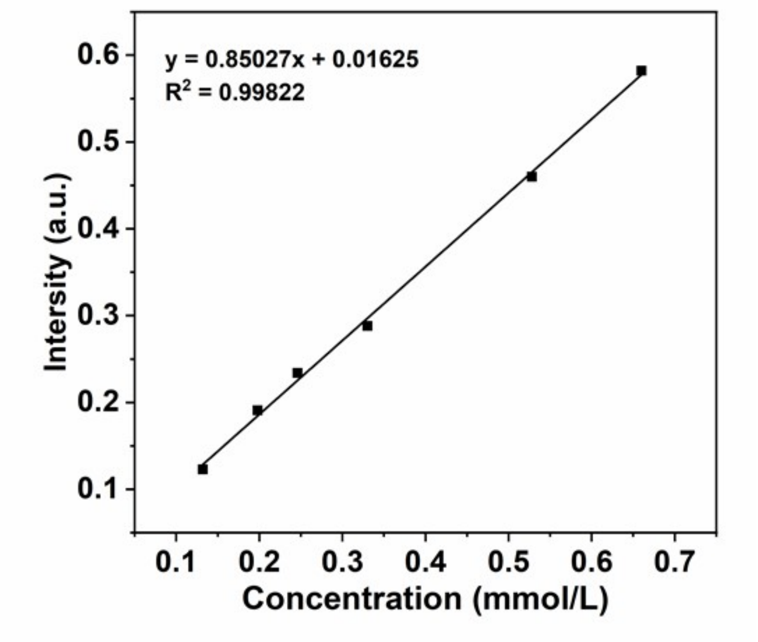

Fig. S18. Calibration curve for iodine concentration determination. The fitted standard concentration curve was obtained by linear regression of experimental data ($R^2 = 0.99822$).

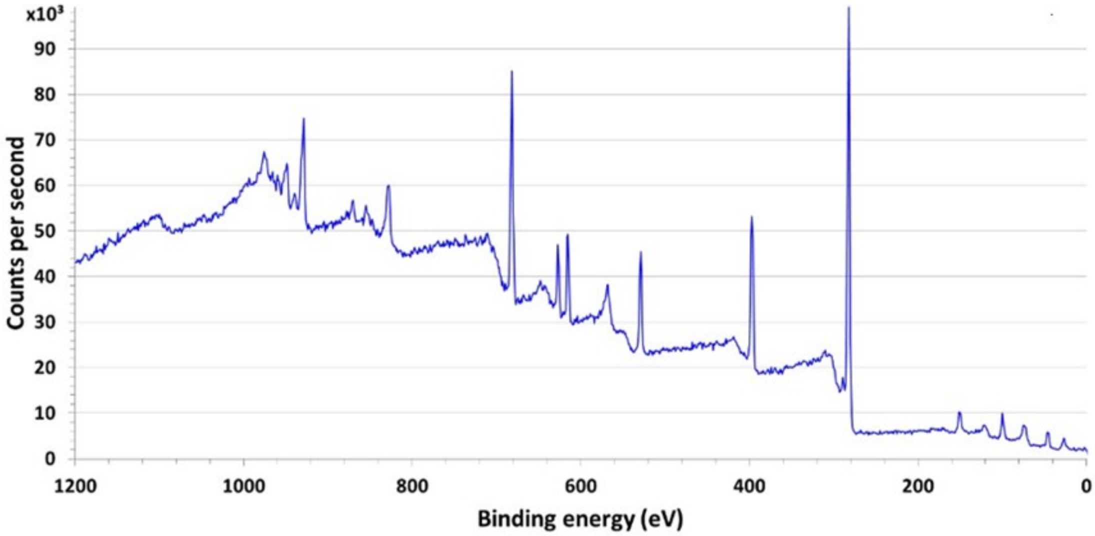

Fig. S19. XPS of **Cu-TMBIB-a**.

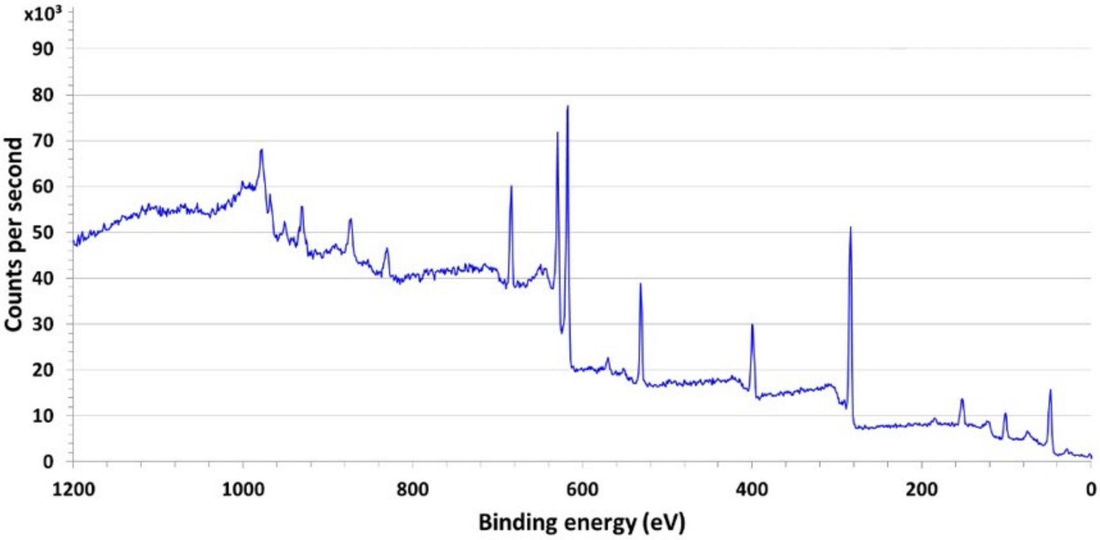

Fig. S20. XPS of **I_2@Cu-TMBIB-a**.

Table S2. List of involved hydrogen bonds in **Cu-TMBIB-a**.

D - H...A	D-H (Å)	H...A (Å)	D...A (Å)	∠D - H...A (°)	
C10--H10..F1	0.9300	2.5300	3.059(4)	116.00	.
C10--H10..F2	0.9300	2.4100	3.326(7)	168.00	.
C10--H10..F2	0.9300	2.4600	3.269(7)	146.00	7_656

Table S3. List of involved hydrogen bonds in **Cu-TMBIB-b**.

D - H...A	D-H (Å)	H...A (Å)	D...A (Å)	∠D - H...A (°)	
C8--H8..F6	0.9300	2.4400	3.165(11)	135.00	2_655
C10--H10C..N10	0.9600	2.5400	3.106(13)	118.00	.
C12--H12..F6	0.9300	2.3000	2.936(14)	125.00	11_555
C14--H14C..N14	0.9600	2.4500	2.997(15)	116.00	11_555
C16--H16..F2	0.9300	2.5500	3.385(12)	150.00	4_565
C18--H18B..N5	0.9600	1.7000	2.569(15)	150.00	11_555
C18--H18B..N6	0.9600	1.8700	2.564(16)	127.00	11_555
C26--H26A..F4	0.9600	2.4900	3.225(16)	133.00	5_555
C26--H26A..F7	0.9600	2.1500	3.059(14)	157.00	6_545
C26--H26A..F7	0.9600	2.4000	3.273(13)	151.00	16_545
C30--H30C..F7	0.9600	2.2900	3.180(10)	154.00	.
C38--H38A..F3	0.9600	2.0600	2.951(13)	153.00	8_555
C38--H38A..F3	0.9600	1.8400	2.799(14)	172.00	14_555
C42--H42A..F3	0.9600	2.2100	3.121(12)	157.00	.

Table S4. Quantification of all element of **I_2@Cu-TMBIB-a**

	BE [eV]	Mass conc. [%]	Error [%]
Si 2p	98.80	10.9	0.35
Cu 2p	929.00	4.6	1.12
N 1s	398.00	11.1	0.34
O 1s	529.20	9.1	0.25
F 1s	682.50	8.6	0.48
C 1s	281.90	35.5	0.66
I 3d	615.50	20.3	0.49

References

[1] G. M. Sheldrick, *Acta Crystallogr. Sec. A* **2008**, 64, 112.

[2] a) P. Vandersluis, A. L. Spek, *Acta Crystallogr. Sec. A* **1990**, 46, 194; b) A. L. Spek, *J. Appl. Crystallogr.* **2003**, 36, 7.